

Thermal Cycling Reliability of Vanadium Dioxide Films for Switching Applications

Department of Electrical and Computer Engineering

Gus Workman

Advisor: Nima Ghalichechian

Abstract

Vanadium dioxide (VO_2) is a phase change material that rapidly changes from an electrical insulator to a conductor at 68 C. Because of this property, VO_2 has recently been applied in different fields as a thermally activated switch. However, while voltage-activated and current-activated reliability studies of VO_2 films have been carried out, the reliability of VO_2 films that undergo thermal cycling has not been extensively studied. In this investigation, a framework for testing this thermal cycling reliability of vanadium dioxide (VO_2) films was created. The test fixture is comprised of several major components, including a wafer with VO_2 films and integrated Joule heater elements, a test controller board for generating configurable PWM waveforms for the heater elements, a mount to secure the board and the wafer together, and software to manage and monitor the thermal reliability study. Simulations were performed using COMSOL Multiphysics simulator to determine the necessary parameters of the heating signal voltage and current that are required to thermally cycle the VO_2 films. The controller board was then designed to be able to provide such a signal, and a printed circuit board (PCB) was created using KiCad. The board was manufactured and assembled, and custom firmware was loaded onto the microcontroller chip to enable communication with a host computer over a USB interface. After establishing the physical dimensions of the controller board, a mount was designed to securely hold the controller board and wafer in contact with each other using spring-loaded pins. Finally, a Python script was developed to operate the controller board from a host computer, including reading out data from the board. Due to the COVID-19 pandemic, wafer manufacturing was significantly delayed, but the functionalities of the test system were verified using a resistor as a simulated load. The board performed to the specifications set by the simulations and was able to output a configurable 16V PWM signal. The framework for testing

thermal cycling reliability developed in this project will be applied to understanding the thermal reliability of vanadium dioxide films, but it can also be easily extended to other reliability studies that involve voltage, current, or thermal activation of the device under test.

Acknowledgements

I would like to sincerely thank my research advisor, Nima Ghalichechian, for allowing me with this opportunity to make contributions on meaningful research and to become more exposed to different areas in electrical engineering. I would also like to thank Mark Lust and Shangyi Chen for mentoring me and working closely with me to complete the goals of the project.

Table of Contents

<i>Abstract</i>	1
<i>Acknowledgements</i>	3
<i>List of Figures</i>	5
<i>List of Tables</i>	6
<i>Introduction</i>	7
<i>Methodology</i>	8
<i>Results</i>	21
<i>Conclusion</i>	25
<i>Appendix A: Controller board circuit schematic</i>	27
<i>Appendix B: Simulated load testing procedure</i>	28
<i>Bibliography</i>	29

List of Figures

Figure 1: Transition cliff of VO ₂ films [2].....	7
Figure 2: AutoCAD drawing of wafer features	9
Figure 3: Unit cell Joule heater COMSOL simulation	11
Figure 4: VO ₂ device fabrication	12
Figure 5: Block diagram of the controller board	13
Figure 6: Microcontroller and current sensor circuit blocks.....	15
Figure 7: USB to UART bridge and voltage regulator circuit blocks	15
Figure 8: Rendering of the controller board design.....	16
Figure 9: Fully assembled controller board	18
Figure 10: Rendering of mount design	19
Figure 11: Fully assembled test fixture.....	19
Figure 12: Screenshot of Python client software	20
Figure 13: Simulated load testing setup.....	22
Figure 14: Current sensor measurements during simulated load testing	23
Figure 15: Oscilloscope verification of 16V PWM waveform.....	24

List of Tables

Table 1: Bill of materials for controller board	17
---	----

Introduction

Phase change materials are materials that undergoes a change in the structure of the material when heated or cooled. Vanadium dioxide (VO_2) is a phase change material that changes in molecular structure when heated, resulting in a change in conductivity property of the material. In Figure 1 below, the resistivity of VO_2 through a range of temperatures is displayed. When heated to 68°C , VO_2 rapidly changes from an electrical insulator with a high resistivity to an electrical conductor with very low resistivity [1]. This period of change is known as the metal-insulator transition region. The non-linear behavior and rapid change from insulator to conductor in just a few degrees observed in VO_2 films allows it to act as a thermally activated switch.

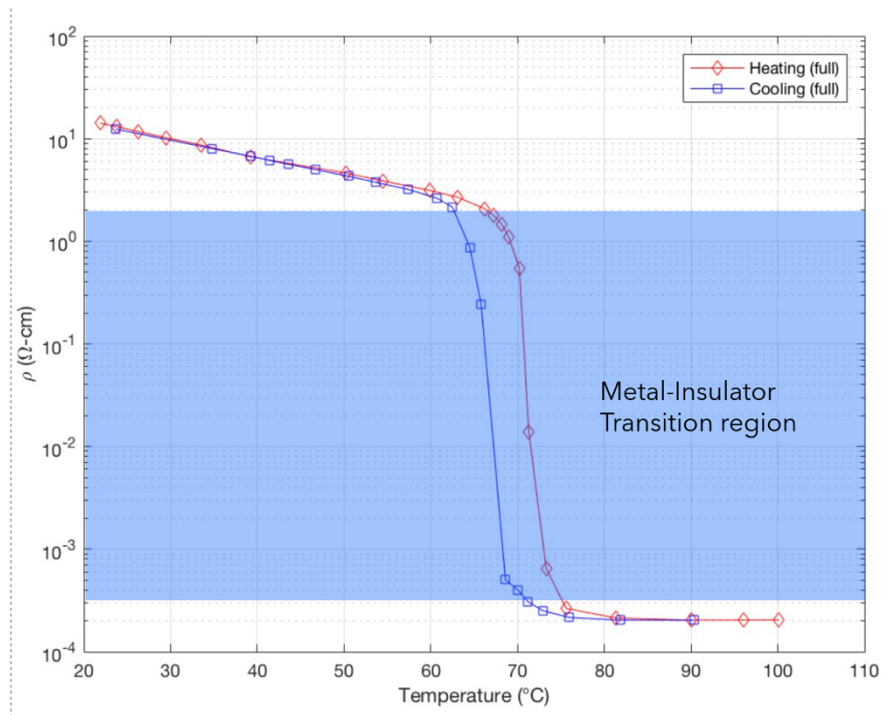


Figure 1: Transition cliff of VO_2 films [2]

Although vanadium dioxide is not the only phase change material that undergoes a change in electrical resistivity at different temperatures, it is of interest to the scientific community because of the relatively low temperature at which the phase change occurs. Other

phase change materials, such as germanium-antimony-telluride (GST) have transition temperatures as high as 618 °C [3]. Because of the relatively low transition temperature, VO₂ has already been utilized in RF applications such as passive imaging arrays in the millimeter wave frequency band [4], reconfigurable high-frequency filters [5], and more.

One aspect of VO₂ that is not yet extensively studied by the scientific community is the reliability and lifespan of VO₂ films when used as a thermally activated switch. Previous studies have been done by the XLIM Research Institute in France, but these were concerning the other activation modes of vanadium dioxide. In the study, the researchers tested the voltage and current activation of VO₂ films and measured the number of cycles required to reach the point of failure of the device. It was found that current-controlled switching of VO₂ devices can last for more than 260 million cycles, while the voltage activated VO₂ devices fail at around 16 million cycles [6]. This study will perform a similar experiment, but instead of focusing on current or voltage activation, thermal activation of the VO₂ films will be studied. The goal of the study is to develop a framework for testing the thermal activation reliability of VO₂ films acting as switches, and to determine the point of failure for these devices.

Methodology

To test the reliability of VO₂ films that undergo repeated thermal cycling, a test fixture was designed. The test fixture consisted of several main components, including a wafer with VO₂ structures, a cycling controller, a mount, and finally custom software to communicate with the test fixture.

A two-inch sapphire was used as the base material for the VO₂ testing structure. Sapphire is commonly used for designing circuits with VO₂ features because of the lattice matching of the VO₂ and the crystalline form of sapphire. This helps give the VO₂ better purity and crystallinity

during manufacturing. The VO₂ and copper structures that were added to the wafer were first designed in AutoCAD. The AutoCAD layout of the structures can be seen in Figure 2.

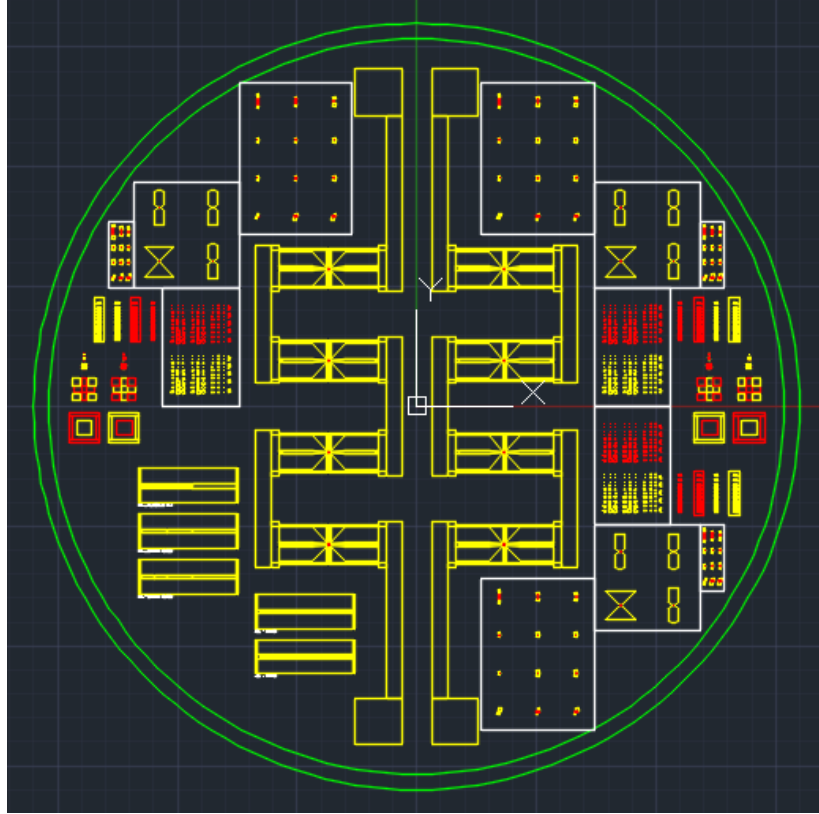


Figure 2: AutoCAD drawing of wafer features

To achieve thermal cycling of VO₂ structures, there are several main components of the designed wafer. First, the VO₂ films are deposited to connect signal to ground coplanar waveguides. The waveguides are important, because it allows the RF signal to pass through or be blocked by the VO₂. To do so, a signal is injected into the waveguide using RF probes on one end of the device under test (DUT) and the resulting signal is read out of the other side. When the VO₂ changes from a dielectric to a conductor, the signal line is short-circuited to ground and the transmission of the RF signals change. When the resistance is in the low state, the RF signals are reflected at the VO₂, and the measured signal at the readout probe is greatly decreased. The second important component is the Joule heater elements adjacent to the VO₂ films. These films

are able to locally heat the VO₂ past the transition cliff, providing a mechanism for control of the conductivity state of the VO₂. The Joule heater elements are simply small traces of copper that heat up when a current is passed through them due to the natural impedance of the copper.

After designing the wafer in AutoCAD, the COMSOL Multiphysics program was utilized to simulate the parameters of the electrical signal applied to the Joule heater elements to ensure that the VO₂ is able to transition to the excited state and back. From the simulation, it was determined that an applied voltage of 4V across each Joule heater element with a current of 0.8A for three milliseconds would be sufficient to entirely heat the VO₂ films to over 100°C, which is well past the transition point. However, for testing thermal cycling reliability, it is also important to ensure that the VO₂ films fully transition back to the relaxed state before thermally exciting again. To ensure that this would not be a problem, COMSOL was used to calculate timing parameters for cooling to ensure that the transition back to the relaxed state would occur. It was determined that seven milliseconds between pulses would be enough to allow the heat to dissipate into the wafer, bringing the temperature of the VO₂ films down to almost room temperature. A screenshot from the COMSOL simulation is shown in Figure 3 below.

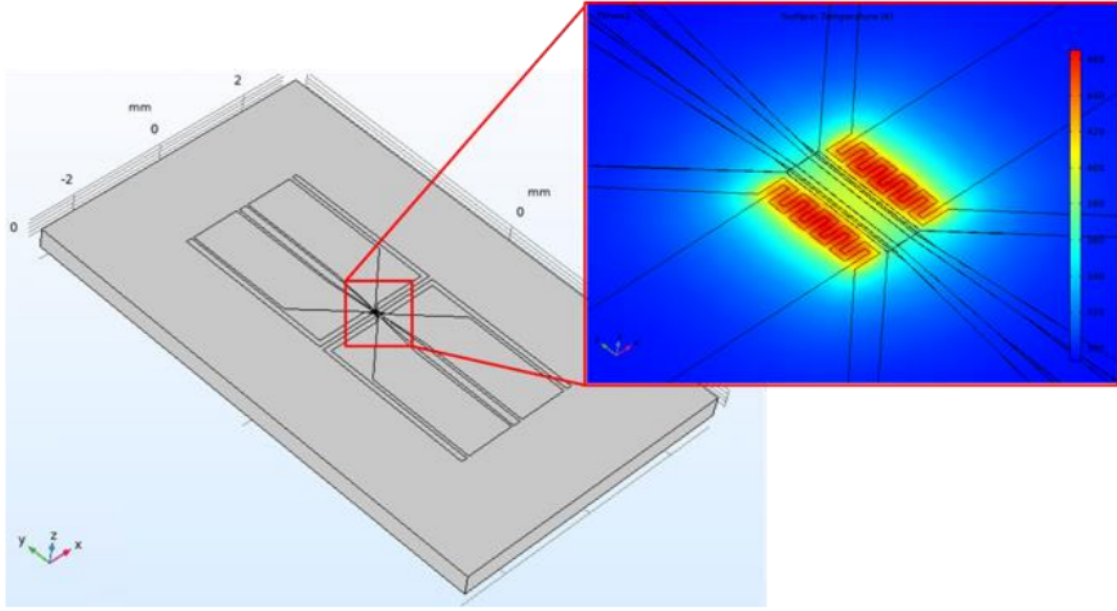


Figure 3: Unit cell Joule heater COMSOL simulation

Another concern that COMSOL simulations were used to address were the possibility that repeated thermal cycling of the films would allow heat to build up in the wafer, to the point where the seven milliseconds between pulses is not enough time to allow the VO_2 films to completely go back through the phase change. However, the simulation performed showed that even after 40 cycles, the given parameters of the pulse to the Joule heater elements are sufficient to prevent such heat buildup from happening.

After designing and simulating the parameters of the wafer, the wafer was manufactured at the Ohio State University NanoTech West facility. The manufacturing is a two-layer process, with the first step involving patterning the VO_2 structures and the second step layering on the copper structures. An etching method involving a photoresist was used, as described in [3]. The general steps are shown below in Figure 4.

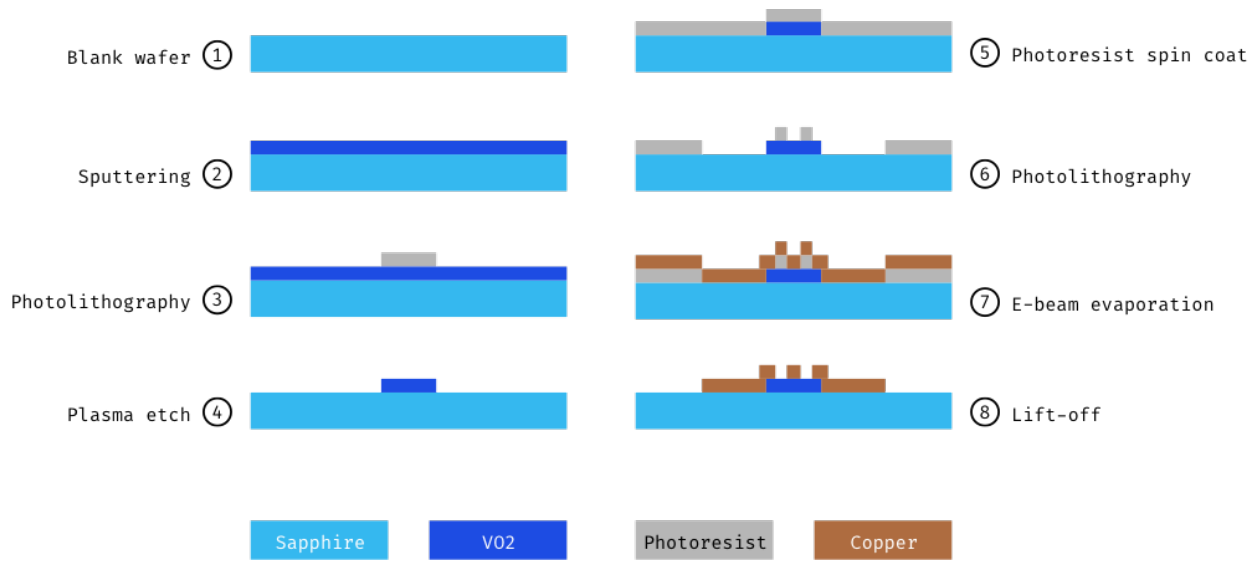


Figure 4: VO₂ device fabrication

In the simplified VO₂ manufacturing process shown above, steps 1-4 show the etching of VO₂ features. To do so, a sapphire wafer is plated with VO₂, then photoresist is used to protect the VO₂ features that should not be etched away. In steps 5-8, copper is added to the design using the lift off process. In this process, photoresist is first patterned for the areas that should not have copper. Then the copper layer is deposited, and the photoresist is stripped, taking the unneeded copper with it.

From the simulation results of an applied three millisecond pulse of 4V and 0.8A for each Joule heater element on the wafer, a controller board was designed. Given that the wafer consisted of eight Joule heater and VO₂ elements, with two parallel sets of four elements in series, the controller board needed to be able to apply and control a 16V signal across the terminals of the Joule heater elements. Additionally, to ensure that the manufactured board met the properties of the simulation, the board was required to have current sensors, which are able to measure the current through the Joule heater elements. The block diagram created from these requirements is pictured below in Figure 5.

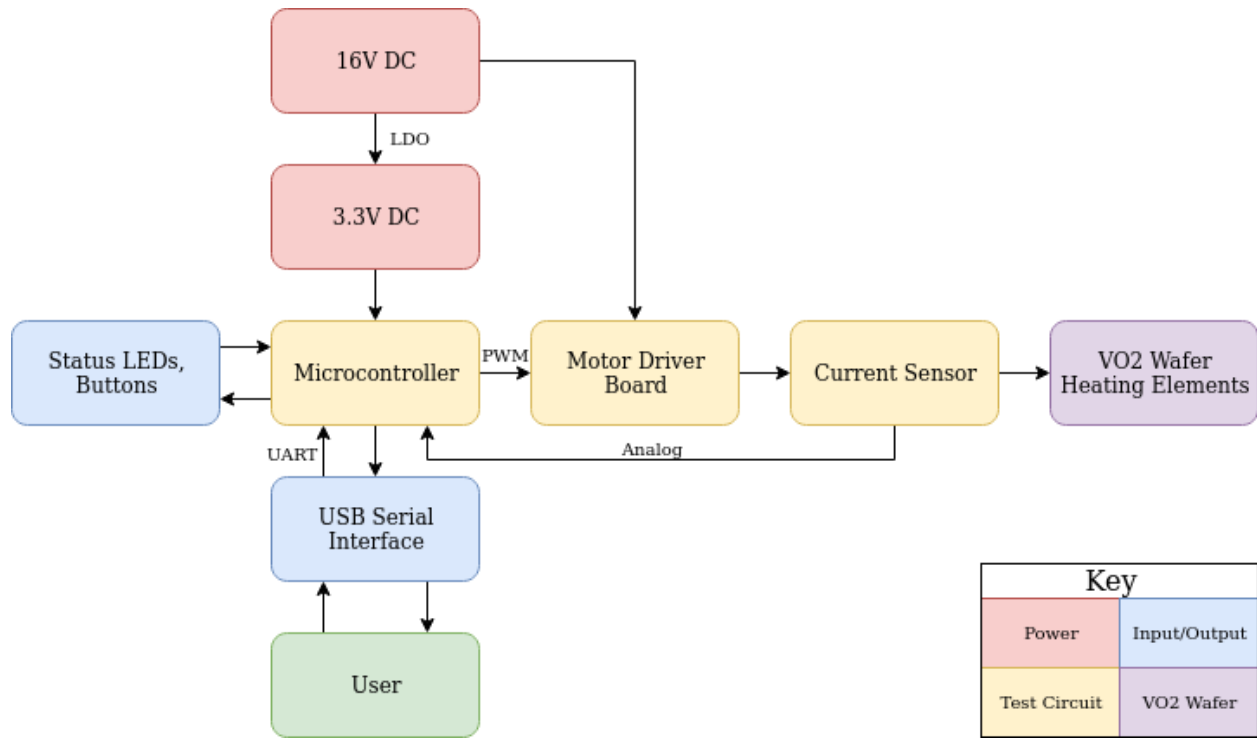


Figure 5: Block diagram of the controller board

From this block diagram, specific components to meet the requirements were chosen. The microcontroller used on the board was the STM32G030. This chip was chosen because of its ease of use and advanced features. This chip requires very few external components to operate correctly, mostly just requiring bypass capacitors to provide a steady power supply. It also has an extensive hardware abstraction layer (HAL) provided by the manufacturer, which greatly simplifies programming the device. Additionally, this chip also includes advanced features, including timer PWM modes with interrupts that allow for efficient and accurate controlling of the 16V pulse and integrated 12-bit analog to digital converters that support direct memory access (DMA) modes for simple and automatic reading of the current sensors.

The downside of the STM32G030 chip is that it does not include onboard USB support, so to administer communication with a host computer, the FTDI230XS chip was utilized. The FTDI2230XS chip acts as a bi-directional UART to USB bridge, translating the UART signals

that the microcontroller can understand into the standard USB signals utilized by modern computers. Adding this bridge to the design provides an interface by which the current state of the board can be monitored.

The controller board also utilized an external motor driver board. This was used to simplify the control mechanism for the 16V signal. The external motor driver board is able to convert a 3.3V logic-level signal output from the microcontroller into the 16V pulse that is required by the Joule heater elements. While this could also be done using a MOSFET as a voltage-activated switch, the use of a motor driver board allows for a higher maximum output current, and it also provides some safety features, including current limiting, thermal shutdown, and overvoltage protection.

After choosing the parts, an electrical circuit schematic was created to represent the electrical connections between each of the pins of the components required to make the board work. The schematic was designed in the program KiCad, which is shown in Appendix A: Controller board circuit schematic. There are four main components of the schematic. First the microcontroller is in one of the center blocks of the diagrams, also shown below in Figure 6a. The microcontroller has connections to the inputs and outputs on other chips on the device. It also features a voltage divider to read the voltage of the power supply, and a number of decoupling capacitors to filter out power supply noise. Another important part of the schematic is the current sensors, as shown in Figure 6b. The current sensors feature inputs and for the 16V signal generated by the motor driver board that goes to the heaters, and an analog output that is routed to the ADC of the microcontroller.

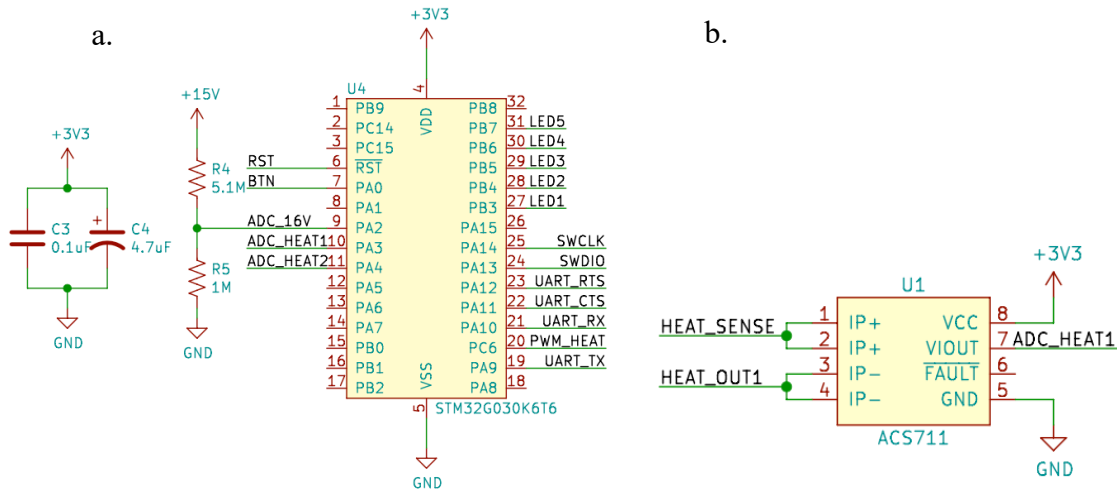


Figure 6: Microcontroller and current sensor circuit blocks

The other two main components of the schematic are the UART to USB bridge and the voltage regulator circuit, which were designed to the manufacturer's recommendation. As shown in Figure 7a, the voltage regulator circuit features an impedance matching circuit for the differential USB signal. For the voltage regulator circuit in Figure 7b, the main power source voltage input is selected using two diodes. This design allows the board to run independently off of the higher voltage 16V input or the lower 5V input from the USB, or a combination of both. By adding the diodes to the design, this allows for easier development since the microcontroller can be programmed without requiring the higher voltage signal.

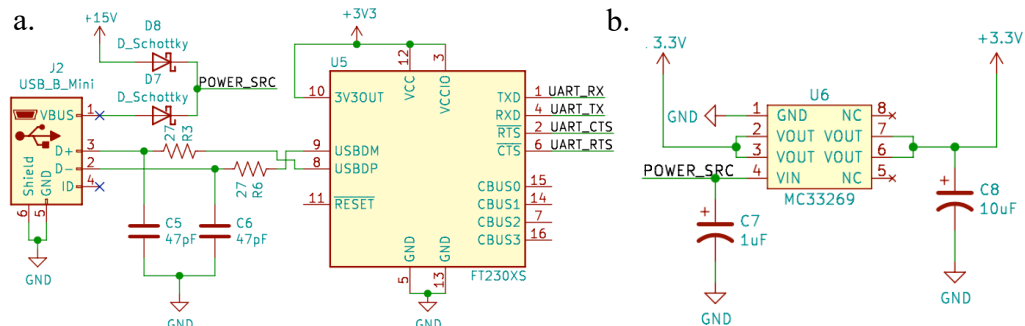


Figure 7: USB to UART bridge and voltage regulator circuit blocks

From the schematic, a 2-layer printed circuit board (PCB) was designed. While laying out the components on the board, special care was taken to follow best practices for circuit design, including minimizing the length of signal traces to reduce noise, using thick traces for high-current signals to prevent heat buildup, and incorporating a ground plane to avoid developing ground loops. Additional features of the board include pads to power the board from a DC power supply via alligator clips, multiple test points to analyze signals, and solder joints to easier enable or disable specific outputs of the board. A rendering of the board is shown below in Figure 8.

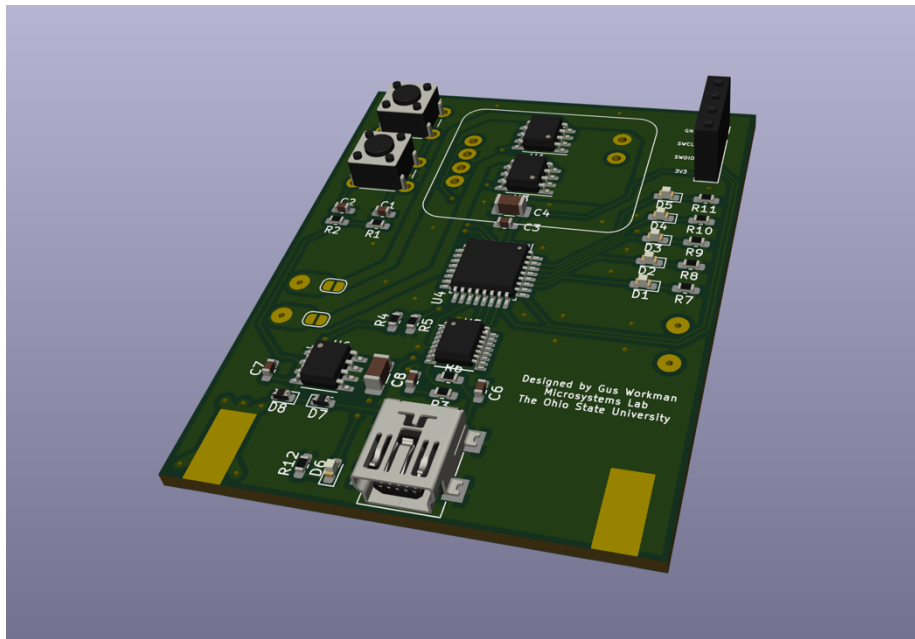


Figure 8: Rendering of the controller board design

After finalizing the design of the board by verifying the manufacturability of the design, KiCad was used to generate Gerber files, which were sent to a board fabrication service to produce. The bill of materials for the board are below in Table 1.

Table 1: Bill of materials for controller board

Reference	Quantity	Value	Purpose
C3 C1 C2	3	0.1uF	Decoupling capacitor
C4	1	4.7uF	Decoupling capacitor
C6 C5	2	47pF	Impedance matching
C7	1	1uF	Filtering capacitor
C8	1	10uF	Filtering capacitor
D5 D4 D3 D2 D1 D6	6	LED	Progress indication
D7 D8	2	D_Schottky	Power supply
J1	1	0.1" Header 1x4	Programming header
J2	1	USB_B_Mini	USB connector
J3	1	VO2_SPRING_PINS	VO2 connect push pins
JP1 JP2	2	SolderJumper_2_Open	Solder jumper
R1 R2	2	100k	Pull up resistor
R3 R6	2	27	Impedance matching
R4	1	5.1M	Source voltage sensing
R5	1	1M	Source voltage sensing
R7 R11 R8 R9 R10 R12	6	500	LED current limiting resistor
SW1 SW2	2	SW_Push	Push button
U1 U3	2	ACS711	Current sensor
U2	1	DRV78871	Motor driver board
U4	1	STM32G030K6T6	Microcontroller
U5	1	FT230XS	UART to USB bridge
U6	1	MC33269	Voltage regulator

After receiving the electrical components from an online distributor and the PCB from the fabricator, the components were soldered by hand onto the board. Most of the components, including the surface mount resistors, capacitors, and the larger integrated circuit (IC) chips, were soldered by hand using a soldering iron, but some of the higher pin count IC components were soldered using solder paste, flux and a hot air gun. The resulting mostly assembled board

appears below in Figure 9, with the only missing components being the add-on motor driver board and the spring pins that connect the wafer and the controller board.

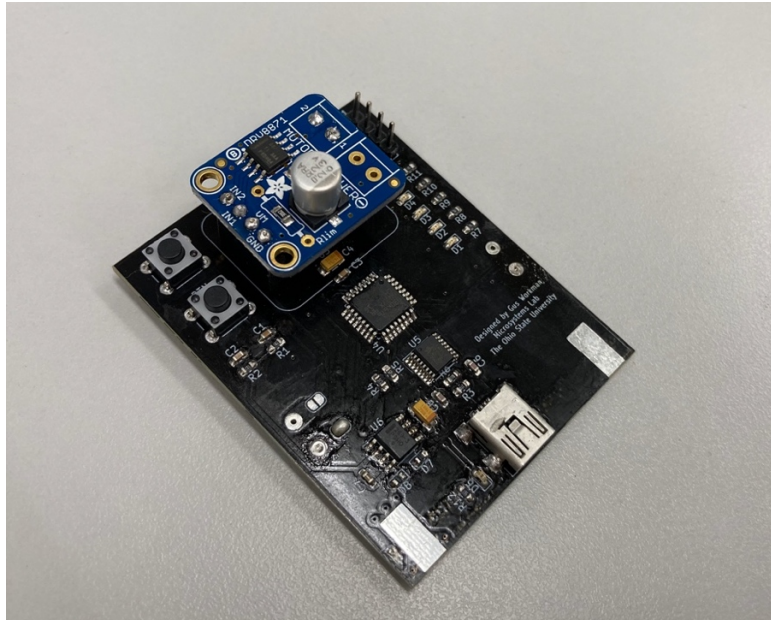


Figure 9: Fully assembled controller board

After finalizing the dimensions of the controller board, the mount was designed in AutoDesk Fusion 360. Given that the spring-loaded contacts that deliver the voltage for the Joule heaters on the wafer are 12 mm long when fully extended and 9 mm long when fully compressed, the mount was designed to hold the controller board and wafer at 10 mm apart. To ensure that the wafer is aligned, the bottom half of the mount has a slightly flat edge at the front, which aligns with the flat edge of the wafer. Additionally, the bottom half of the mount features a cutout which allows for the use of the wafer tweezers for inserting and removing the wafer into the holder. To ensure that the wafer and board are securely connected, the mount features a hole in each of the support posts for heat-set threaded inserts that enable the use of screws to hold the two mount pieces securely together. The screw holes can be seen in the rendering of the mount in Figure 10 below.

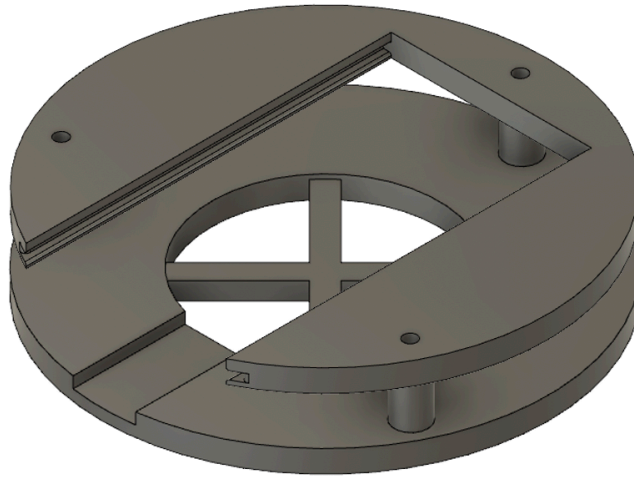


Figure 10: Rendering of mount design

After assembling the controller board, printing the mount, and manufacturing the wafer, the final system was tested together to ensure the fit. While the height between the wafer and the board was just right, the diameter for the cutout to hold the wafer was just a little too small and required some sanding before the wafer fit. The final assembled system is shown in Figure 11.

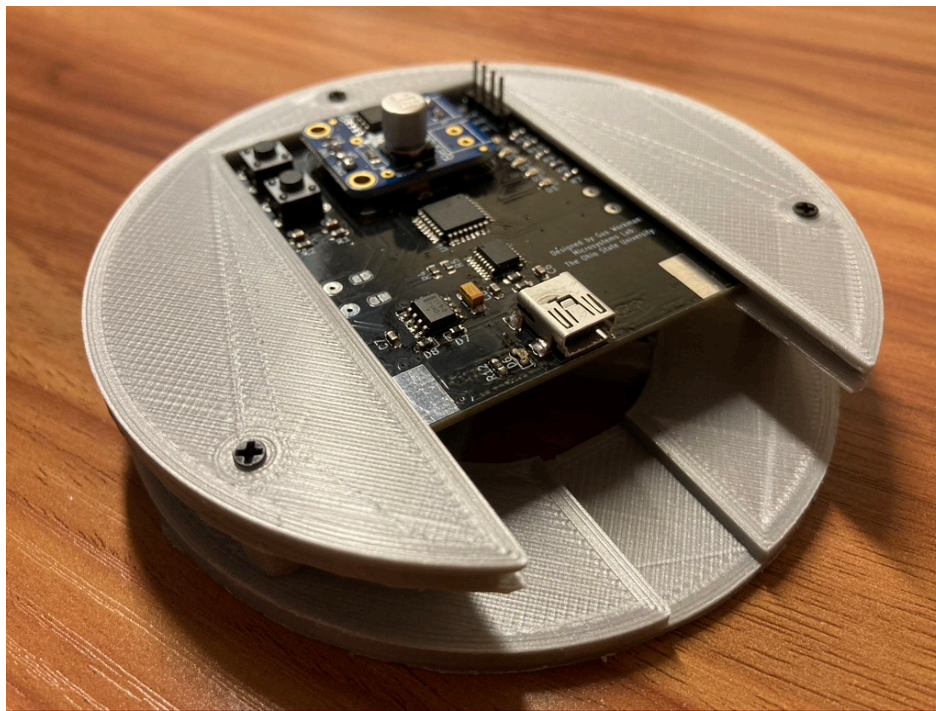
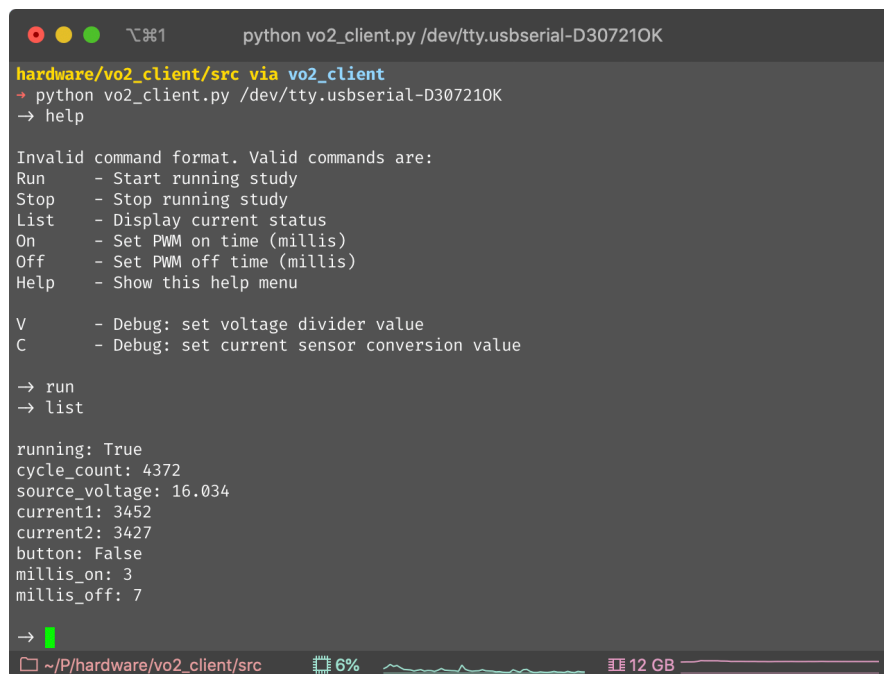


Figure 11: Fully assembled test fixture

One of the final components for this study is the software and firmware required to control the device. To program the STM32G030 microcontroller, the STM32 HAL libraries were used. The device was programmed in C, and the community-developed stlink tool was used to upload the compiled firmware files to the microcontroller. The firmware utilized timers for PWM generation to control the heaters, UART and interrupts to communicate with the computer, and the built-in ADC peripheral with DMA to sample the current sensors. A client controller software was developed in Python, to aid with controlling and reading out the data of the microcontroller. This software used the serial port to send commands to the microcontroller. The program uses the asyncio library to asynchronously run several different tasks, including reading user input and monitoring current state of the system. It also includes several options for debugging and tuning parameters on the board. A screenshot of the program is included in Figure 12 below.



```
python vo2_client.py /dev/tty.usbserial-D307210K
hardware/vo2_client/src via vo2_client
→ python vo2_client.py /dev/tty.usbserial-D307210K
→ help

Invalid command format. Valid commands are:
Run      - Start running study
Stop     - Stop running study
List     - Display current status
On       - Set PWM on time (millis)
Off      - Set PWM off time (millis)
Help     - Show this help menu

V        - Debug: set voltage divider value
C        - Debug: set current sensor conversion value

→ run
→ list

running: True
cycle_count: 4372
source_voltage: 16.034
current1: 3452
current2: 3427
button: False
millis_on: 3
millis_off: 7

→
```

Figure 12: Screenshot of Python client software

Results

Due to the COVID-19 pandemic, the results of this project have been delayed. While the reliability testing was originally scheduled to start in late spring and carry into the fall of 2020, the COVID-19 pandemic slowed down progress on wafer fabrication. Because the NanoTech West facility was closed from March until autumn, testing could not start when originally planned. After reopening, the wafer fabrication process experienced some issues with aligning the mask for the photoresist, causing further delays.

After manufacturing the first wafer in October 2020, the measured resistance of the Joule heater elements was significantly higher than the simulated values, at about twice the resistance. The differences seen in the manufactured wafer and the simulation are likely because the conductivity of the copper is lower than was expected. This could be due to impurities in the copper.

To combat this issue, additional wafers with an updated design to account for the different conductivity will be manufactured for testing. In order to speed the process up, preliminary testing will occur by shorting two of the Joule heater elements out of the circuit, such that only two of the four Joule heaters on each side of the test fixture actually pass current through them. This will reduce the overall resistance of each of the heater traces and will keep the voltage necessary to produce the required heating current within the range that the controller board can handle.

In lieu of having the manufactured wafers to perform testing with, simulated load testing was done to ensure that the controller board and software were working correctly. To do so, a simulated load was applied across the output terminals of the board in place of where the Joule

heater elements would be in the wafer circuit. The procedure found in Appendix B: Simulated load testing procedure details the process that was used to verify the current sensors, PWM signal, and the stop condition of the board. An image depicting the oscilloscope connections and simulated load are found below in Figure 13.

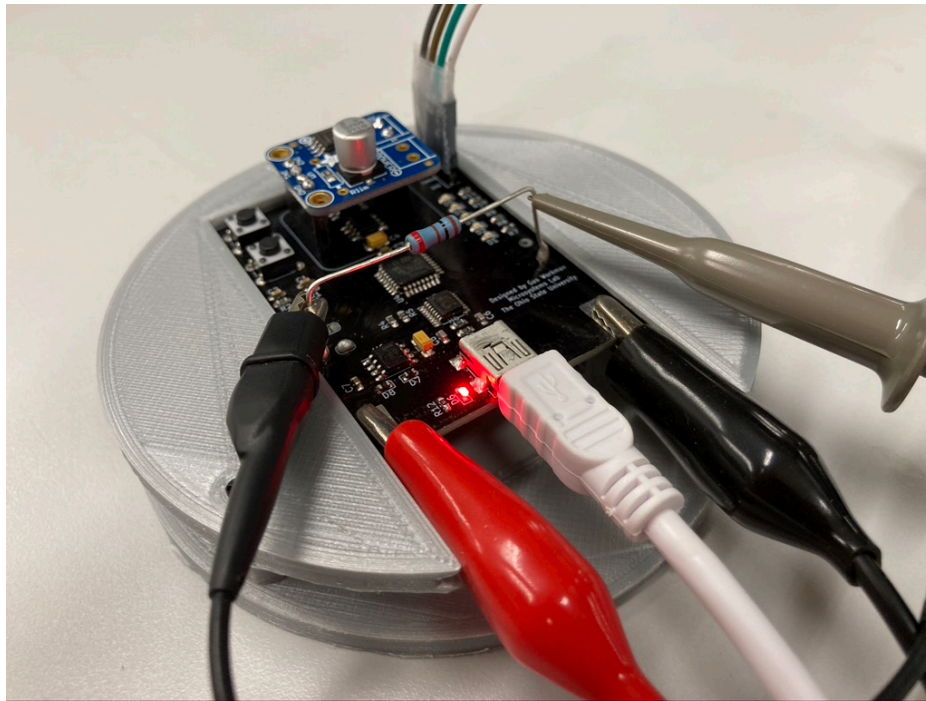


Figure 13: Simulated load testing setup

To ensure the current sensors were reading correct values, the measured current value during the pulse and between pulses was output. The expected values were 0.16A during the pulse and 0A between pulses. However, the current sensors experienced several issues that reduced the usability. First, the current sensors had the issue of not being sensitive enough to the currents produced by the test load. The ACS711 were chosen for the board because of the easily hand-solderable form factor and low price, but these sensors have a sensing range of -12.5A to 12.5A, which is much greater than the necessary 0A to approximately 3A needed for this project. This means that the sensors are not very well suited for accurately reading smaller currents, such as the 0.16A produced by the simulated test load. Even after calibration, the standard deviation

of the signal at 0A was 0.032A, which is an obstacle in drawing any conclusions from the current sensors. However, another big problem is that the firmware of the microcontroller is not optimized for reading and sending current sensor data to the host computer. The fastest that the microcontroller is able to send data is one status packet (which includes the running state, current sensor values, pulse high and low time, error codes and more) every five milliseconds. Because the period of the heater PWM signal is ten milliseconds, this enables at most two samples per period, which is not a sufficient number of samples per period to analyze the current in the time domain to confidently verify the simulations. Figure 14 below shows the measured current sensor output during PWM signal generation.

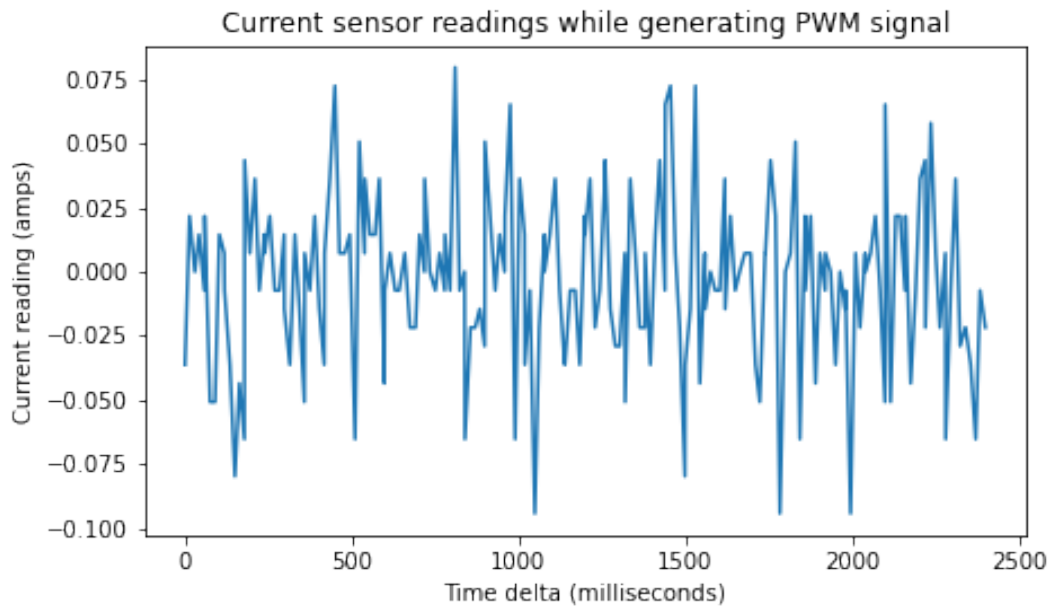


Figure 14: Current sensor measurements during simulated load testing

There are several possible steps that could be taken to address these shortcomings of the current sensors. The first and easiest is to optimize the software to save more ADC samples, and to send them to the host computer at a faster rate. At higher sampling rates and the higher load currents of the actual testing process, the signal would be more distinct and easier to compare

with simulated values. An additional change that could be made is to use more sensitive current sensors, with a sensing range that is closer to the design specifications. This will provide more accurate data, which should have less noise.

An additional aspect of the design verification includes assessing the validity of the output PWM signal, which was observed using an oscilloscope measuring the voltage across the resistor of the simulated load. The signal that was captured can be seen below in Figure 15. The oscilloscope output includes measurements of the pulse width, signal period and peak to peak voltage. These measurements show that the resulting output is very close to expected, with a pulse width of 3.20 ms, a period of 10.6 ms (which corresponds to 7.4 ms at the low voltage) and a peak-to-peak voltage of 15.8 V. The slight discrepancy between the programmed values and the measured values is likely because of the inaccuracies of the internal clock of the microcontroller, which can vary greatly with temperature. Including an external oscillator in a future revision would result in more accurate timings. However, given that both the pulse and rest time is slightly longer at room temperature, the effect should be minimal.

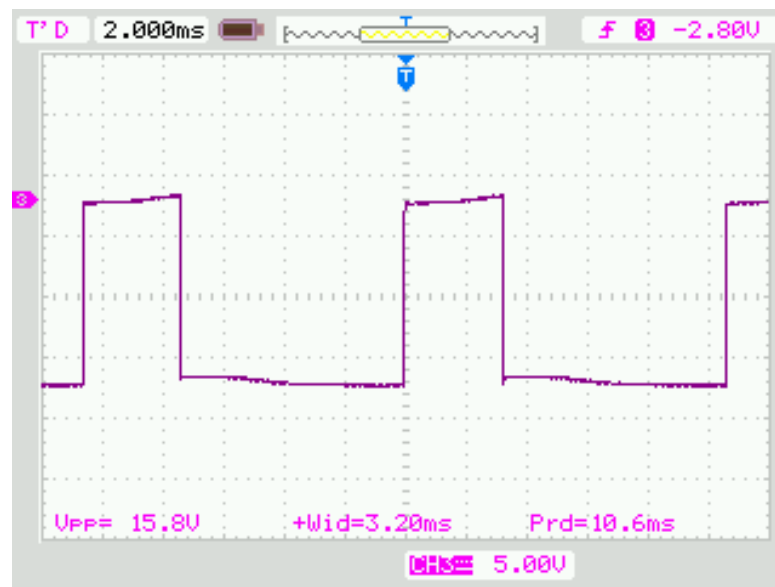


Figure 15: Oscilloscope verification of 16V PWM waveform

Finally, stop condition was ensured to be working correctly by setting a stop condition of 10,000 cycles. After starting the study and letting it run for the 10,000 cycles, the status of the board was checked to ensure that the board had automatically stopped PWM generation. This was confirmed, and additional verification as done by timing the duration of PWM generation. For 10,000 cycles at a period of 10.6 ms, the duration of the heater signal generation by the microcontroller is 106 seconds. The duration was measured using a stopwatch application on a smartphone while observing the output from the oscilloscope, and the recorded duration of PWM generation was 106.89 seconds. This shows that the microcontroller is successfully able to measure the number of cycles and stop after the programmed value.

After performing the simulated load testing, it was determined that the controller board was generating the PWM heater signal as expected. Testing VO₂ reliability using the re-manufactured wafers will occur after publication of this document, with a projected completion date for the study to be in mid-December 2020. The degradation of the performance VO₂ will be measured using RF probes. Testing will occur while the VO₂ is in both the thermally activated and inactivated states. The transmittance of the VO₂ switch will be measured by injecting a 40 GHz signal from the sourcing RF probe, and the output signal will be measured with the reading RF probe.

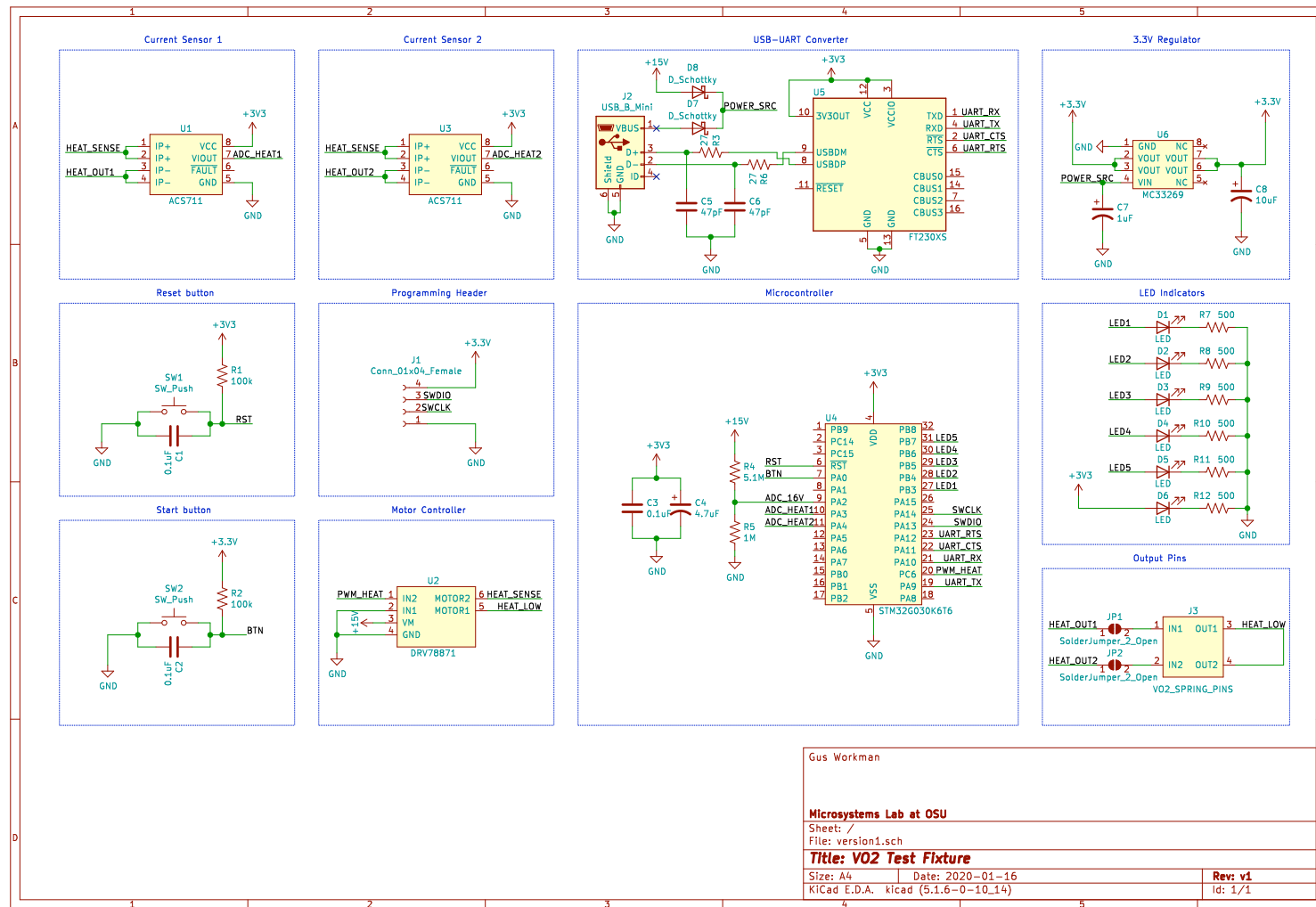
Conclusion

This study involved the creation of a framework for measuring the thermal reliability of VO₂ films used in switching applications. A test fixture was designed and implemented to meet the goals of the study. Although the project experienced delays in manufacturing wafers due to the COVID-19 pandemic, the viability of the system to complete the reliability study was proven

through the simulated load testing. The controller board was able to generate a 16V PWM signal, perform a limited amount of measuring current through the DUT for verifying simulations, and stop the thermal cycling after reaching the user-configured cycle count. The testing framework designed for this project makes it easier for future studies of this nature to be carried out, as testing voltage or thermal cycling of a design will simply require a wafer with electrical contacts in the appropriate location. The input voltage of the design is configurable up to 20V, and so the design can be tuned in different ways to meet the needs of many different types of reliability studies.

Measuring the degradation of VO₂ films after thermal cycling is projected to be completed in mid-December 2020. The steps that will be taken to finish the project include working with the wafer design to ensure the heating elements are able to cause the VO₂ to undergo transition, measuring the baseline RF transmission and reflection at 40 GHz, performing the thermal cycling study, and determining the change in the RF transmission and reflection at various stages of the thermal cycling process.

Appendix A: Controller board circuit schematic



Appendix B: Simulated load testing procedure

1. Solder a 100-ohm resistor across the output terminals of the controller board
2. Attach the leads of an oscilloscope across the terminals of the resistor
3. Power the controller board with 16V from a DC power supply
4. Plug the USB cable from the controller board into a computer that has the client software
5. Using the client software, set the maximum cycle count to 10,000
6. Start the study by sending the run command through the client software
7. Using the oscilloscope, verify that there is a 16V PWM signal across the terminals of the resistor, with a duty cycle of 10 milliseconds and a pulse duration of 3 milliseconds
8. Use the client software to monitor the values being read out of the current sensors. The values should alternate between about 0.16A and 0A
9. Time the study to ensure that the software stops after 10,000 cycles, about 100 seconds

Bibliography

- [1] D. Anagnostou, T. Teeslink, D. Torres and N. Sepúlveda, "Vanadium dioxide reconfigurable slot antenna," in *2016 IEEE International Symposium on Antennas and Propagation (APSURSI)*, Fajardo, 2016.
- [2] OSU RF Microsystems Group, "Phase Change Materials for RF Microsystems," [Online]. Available: <https://microsystems.osu.edu/research/phase-change-materials-rf-microsystems>. [Accessed 15 October 2020].
- [3] M. Lust, S. Chen, C. Wilson, J. Argo, V. Doan-Nguyen and N. Ghalichechian, "High-contrast, highly textured VO₂ thin films integrated on silicon substrates using annealed Al₂O₃ buffer layers," *Journal of Applied Physics*, vol. 127, 2020.
- [4] S. Chen, M. Lust and N. Ghalichechian, "A Vanadium Dioxide Microbolometer in the Transition Region for Millimeter Wave Imaging," in *2019 IEEE International Symposium on Antennas and Propagation and USNC-URSI Radio Science Meeting*, Atlanta, 2019.
- [5] V. Sanphuang, N. Ghalichechian, N. Nahar and J. Volakis, "Reconfigurable THz Filters Using Phase-Change Material and Integrated Heater," *IEEE Transactions on Terahertz Science and Technology*, vol. 6, no. 4, pp. 583-591, 2016.
- [6] A. Crunteanu, J. Givernaud, J. Leroy, D. Mardivirin, C. Champeaux, J.-C. Orlianges, A. Catherinot and P. Blondy, "Voltage- and current-activated metal–insulator transition in VO₂-based electrical switches: a lifetime operation analysis," *Science and Technology of Advanced Materials*, vol. 11, no. 6, 2010.